Enhancing understanding of pulsations in flares using LYRA observations

Report by Andrew R. Inglis (NASA Goddard Space Flight Center)

1. Overview and aims of the project

LYRA provides us with a powerful new tool to investigate the fundamental mechanism behind quasi-periodic pulsations (QPPs) and hence understand the fundamental properties of flare sites. The aim of the project was therefore to use LYRA in tandem with other solar instruments such as AIA, EVE and RHESSI to investigate this phenomenon and thus understand QPP in this context. In particular, two main avenues of research were pursued:

1) The recent work of Dolla et al. (2012) suggests that there may be consistent time delays between QPP observed at different wavelengths during flares. In their study, delays of several seconds were found between the radio, EUV and X-ray signatures of QPP during the 2011 February 15 flare. However, this correlation and time delay has not yet been investigated as a function of time. LYRA flare data represents an ideal opportunity to carry out such an investigation. Systematic changes in the lag between wavelengths as a function of time during flares may yield important insights into the QPP mechanism, and the location and movement of emission sources.

2) Recently, it has become clear that 'red noise' (or frequency dependent noise) effects are an important consideration if QPP signatures are to be correctly interpreted (Vaughan 2005, Gruber et al 2011). If red noise effects are not accounted for, this can lead to the erroneous detection of periodic signals in data that are instead manifestations of signal memory, which leads to higher power at low frequencies. The high temporal cadence of LYRA provides an excellent opportunity to investigate the Fourier spectral properties of flares and the significance of red noise on QPP detection methods.

The ultimate goal of this guest investigation was to perform these investigations on a large sample of solar flares observed jointly with LYRA and RHESSI. By pursuing the above goals we will gain further insights into the structure of flares and the nature of energy release sites. Current progress and results are described in the following sections.

2. Data preparation and treatment

The preliminary stage of this study identified 111 solar flares that were co-observed by the LYRA and RHESSI instruments between 2010 and late 2012. The data for these events was collated from both of these instruments, thus providing a large dataset with the desired high time resolution EUV and X-ray time series data for studying QPP.

2.1 Large-angle rotations (LARs)

Of key importance in time series analysis with LYRA is the correct treatment of the large-angle rotations (LARs) of the Proba-2 spacecraft. Occurring 4 times per orbit, these rotations can generate substantial artifacts in the LYRA time series data. However, utilising the newly available LYRA timeline annotation file (LYTAF), the temporal locations of every LAR can be determined. For this purpose, an automated script was written, which will identify any LARs present in an input LYRA time series by querying the LYTAF. The time intervals corresponding to the LARs are removed, and the remaining time series data is split into sub-intervals to maintain evenly spaced data. An example of this procedure is shown in Figure 1.

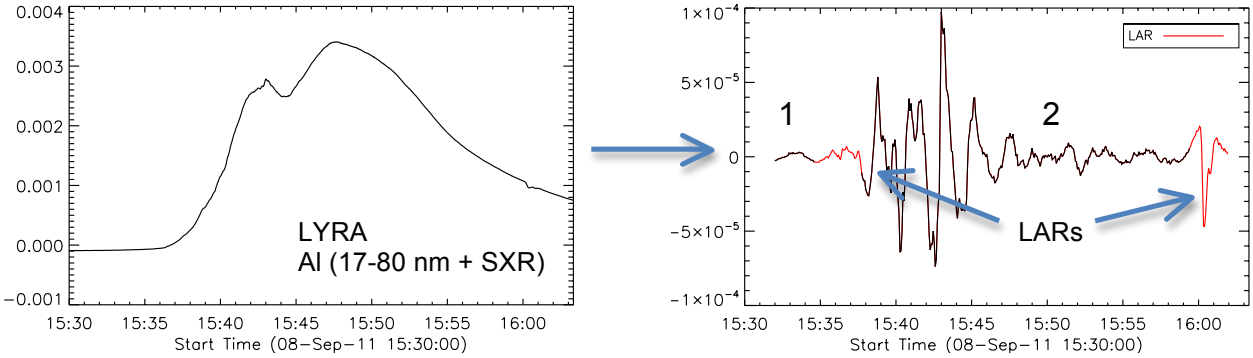

Figure 1 – Automatic identification of LARs in a LYRA time series and splitting of that series. Here the method has been applied to the flare of 2011 September 8. Left panel: The original time series from the LYRA Al filter. The effects of the LAR are visible at 16:00 UT but not pronounced. Right panel: Band-pass filtered LYRA Al data for the same time interval. The red regions indicate the times affected by a LAR. In the filtered data, the effect of the LAR on the time series is much more apparent. The remaining times are split into sub-regions of 'good data', represented by the black lines. In this example there are two LARs and two sub-regions, denoted by '1' and '2'.

Hence, by analyzing each sub-interval returned by the splitting procedure, the LYRA data can be Fourier analyzed with the instrumental artifacts produced by the LARs removed.

The current versions of these scripts are available in IDL format, and take the form of two main modules. First, `search_for_lars` is a function that will query a local copy of the LYTAF database to find occurrences of LARs (and other events such as SAA occurrences) within a specified time window, and return a relevant IDL structure. The second module is `split_series_using_lytaf`, which will take an input LYRA time series, and the structure from `search_for_lars`, and perform the splitting procedure described above and illustrated in Figure 1.

These modules remain in development, but will be made available in their current state as complementary material to this report.

3. Correlation persistence mapping

Here, we introduce the technique of correlation persistence mapping (CPM). The purpose of this method is to investigate the variation of correlation between variables as a function of time. This can be used to investigate the lag between QPP at different wavelengths during flares. As Dolla et al. (2012) recently demonstrated, for some flares there exist time lags between observed pulsations at different wavelengths. Since our understanding of how flare emission is generated at many wavelengths is quite robust, observations of consistent changes in lag time between pulsations at - for example – EUV, soft X-ray and hard X-ray wavelengths could provide important information about the relationship between different emission sites in QPP flares. This information can be combined with other recent studies of the correlation between QPP and other measureable flare arcade parameters such as footpoint separation and, motion, and thermal source location (e.g. Inglis & Dennis 2012, Inglis & Gilbert 2013).

In correlation persistence mapping, the cross correlation for two equal-length time series S_1 and S_2 is found in a specified window, with width w, where $w < N$, the number of elements in S_1 and S_2. For this window, a range of lags L is considered, and the correlation C at each L is found. This process is then repeated for the full time series by sliding the window along the time series, until the end of the series is reached. In this way we build up a map of the correlation between S_1 and S_2 as a

function of t and L. The choice of both w and L is flexible; any value of w may be used, provided that the window width chosen is less than the length of the time series, while any desired range of lags may be investigated. In reality, w should be sufficiently wide as to determine whether there is correlation between two signals for any significant time, while the choice of L is informed by the characteristic timescale that is being investigated.

3.1. Synthetic example of CPM

To illustrate the behaviour of correlation persistence maps, we briefly apply this technique to synthetic signals with a range of properties in Figure 2. The left column compares two signals that are initially in phase. A frequency modifier is introduced to signal 2 at t=100s, leading to a rapid decorrelation. The centre column compares two signals that have a constant phase shift, or time lag, between them. The right column compares two signals that are correlated, but with a changing characteristic lag as a function of time.

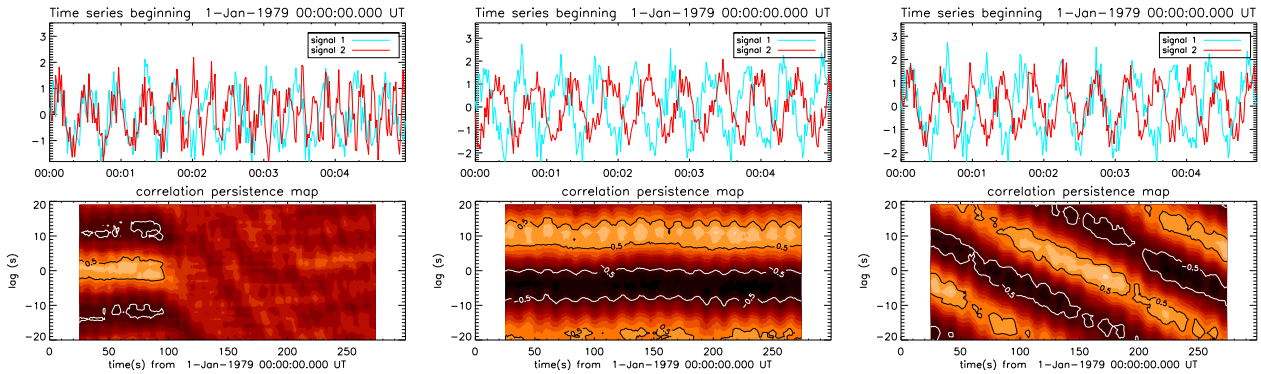

Figure 2 – examples of correlation persistence mapping (CPM) applied to synthetic time series. Left column: two oscillatory signals, initially in phase but de-correlating after t = 100. Center column: two oscillatory signals with a constant phase shift between them. Right column: two oscillatory signals with a linearly changing phase difference as a function of time.

Under these controlled conditions the technique performs well, reproducing the known correlation properties between the two signals. This makes its application to real solar data, where the relationship between two signals is unknown *a priori*, promising.

3.2 Practical example of CPM

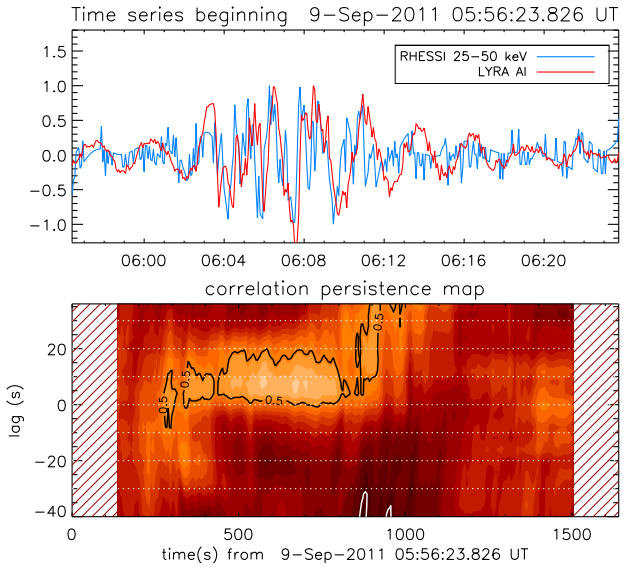

Figure 3 – example of correlation persistence mapping applied to the solar flare of 2011 September 9.

As an example of the practical application of CPMs to the problem of quasi-periodic pulsations, Figure 3 shows an example of this technique applied to data from the 2011 September 9 solar flare. Here we investigate EUV and soft X-ray emission from the LYRA Al filter (Figure 3, red line) and 25-50 keV hard X-rays observed by RHESSI (Figure 3, blue line). As an initial step the data is treated using a bandpass filter, where the range of allowed frequencies is $0.0055 < f < 10.0$ Hz. This is one approach for removing long-term trends in a flare signal that may mask smaller scale variations of interest. Subsequently, the correlation persistence map is applied to the two time series. The result is shown in the bottom panel of Figure 3.

In this example the CPM shows that the RHESSI and LYRA data are strongly correlated between 06:00 – 06:10 UT, with the lag remaining largely constant. Beyond 06:10 the signals de-correlate sharply.

In future work correlation persistence mapping will be applied to a larger sample of flares drawn from our 111-event database, and a wider range of wavelengths will be investigated, thus building on the conclusions drawn by Dolla et al. 2012.

4. Red noise spectra

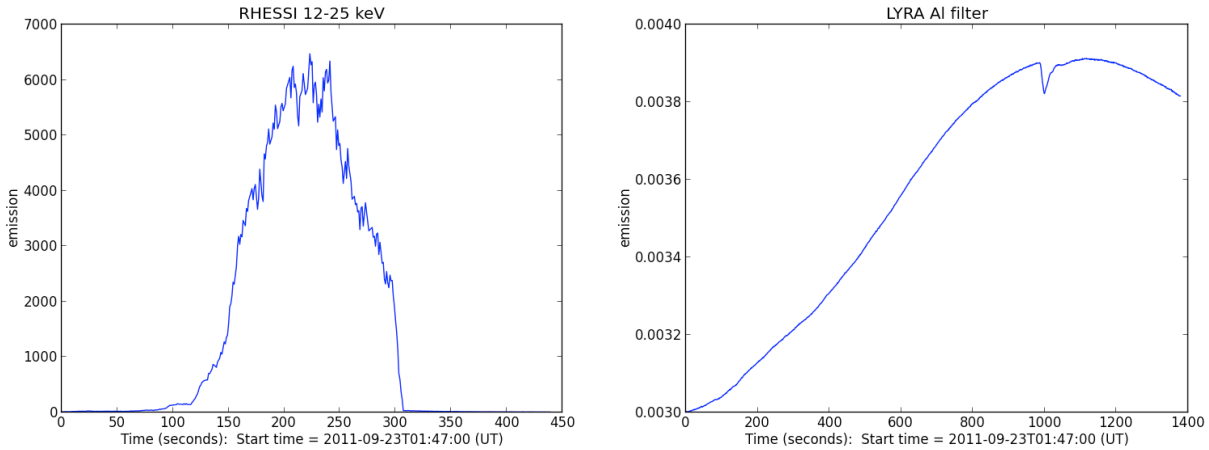

Figure 4 – Time series data from the solar flare of 2011 September 23 as observed by RHESSI (left) at 12-25 keV, and LYRA in the Al filter (right). Not the much shorter time range of significant emission in the RHESSI data, leading to a coarser Fourier spectrum (see Figure 5).

Although the work remains ongoing, the main initial finding of the Guest Investigation was that red noise effects indeed play an important role in the study of solar flare time series. It will be critical therefore to consider this effect in future (and indeed past) studies of QPP. As an example, Figure 5 illustrates the Fourier spectrum observed by LYRA and RHESSI during one of the 111 flares in our event list, the flare of 2011 September 23.

Here the LYRA data have been binned into intervals of 1s to improve the signal to noise ratio. The Fourier spectrum of the flare time series is then determined. In each panel the solid line shows the expectation noise level from a Gaussian noise spectrum (i.e. invariant in amplitude as a function of frequency). Both the Al and Zr channels from LYRA are well fit by a power law spectrum added to a constant (top panels). For each channel the slope of the spectrum is found to be just above 2. Hence it can be seen that the noise level covers several orders of magnitude across the observed frequency range.

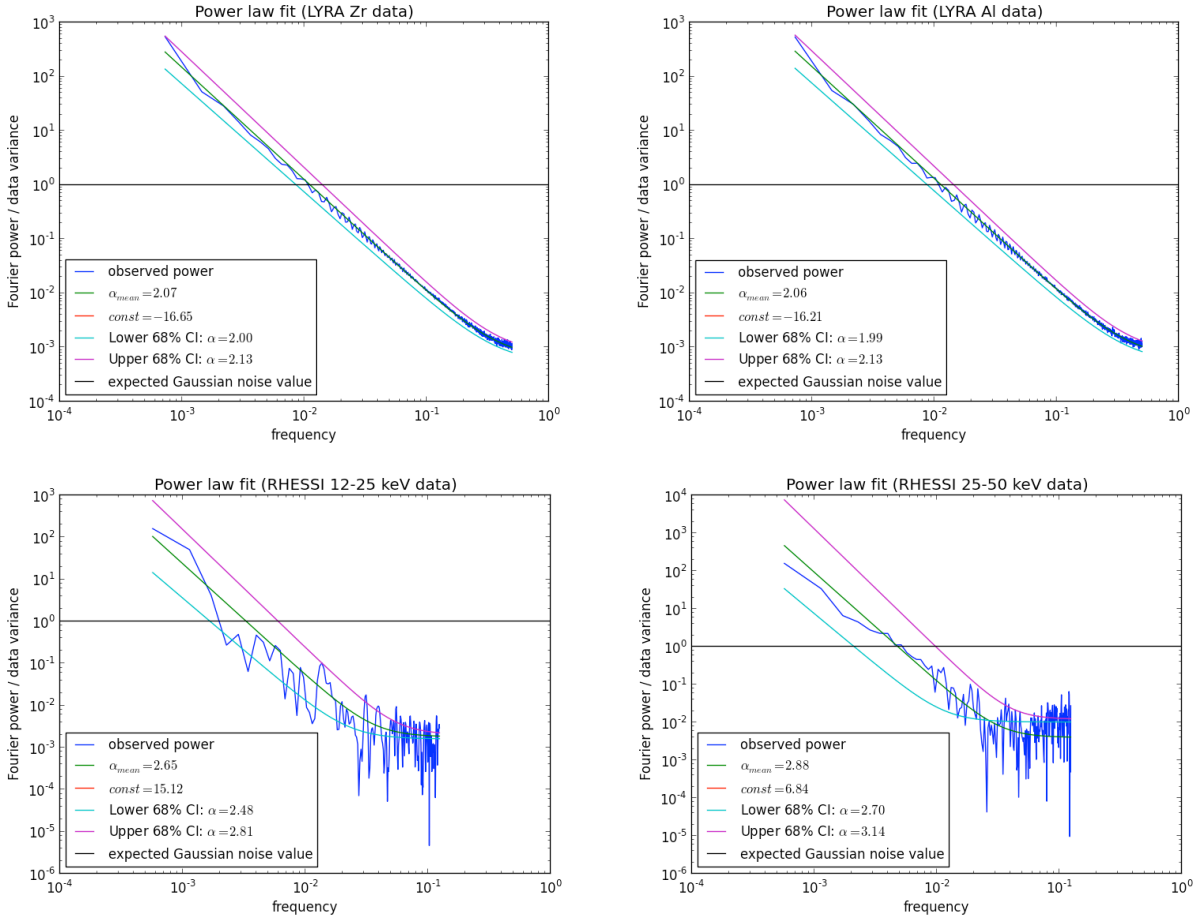

Figure 5 – Fourier spectra of LYRA and RHESI observations of the 2011 September 23 solar flare. Top left: LYRA Zr channel spectrum. Top Right: LYRA AL channel spectrum. Bottom left: RHESSI 12-25 keV spectrum. Bottom right: RHESSI 25-50 keV spectrum. In all cases the Fourier spectrum is visualized on a log-log scale, hence a straight line indicates a power law. Each spectrum is fit using a power law + constant model as shown by the solid green line. The upper and lower 1-sigma bounds are represented by the purple and cyan lines respectively.

The Fourier spectra of 4s-binned RHESSI data are shown in the bottom panels of Figure 2, in the 12-25 keV (left) and 25-50 keV (right) ranges respectively. Although the situation is less clear than for the LYRA data, the RHESSI X-ray Fourier spectrum also shows evidence of a power law component at low frequencies. In both channels there appears to be a transition to a Gaussian 'white noise' spectrum at higher frequencies.

To date, similar measurements have been carried out for approximately 30 flares in the event list, with similar results produced in the majority of cases. The power law slope behaviour of the flare spectra is particularly consistent in the LYRA data, with a mean slope of a ~ -2.1, while RHESSI data are less clear, but also show evidence of a power law component in many cases.

Hence, it is clearly demonstrated that red noise Fourier spectra are a critical component of solar flares at in EUV and X-ray wavelengths, both of which are associated with QPP observations. The detection of power-law Fourier spectra in flares is not new in itself (e.g. Aschwanden et al. 1998, McAteer et al. 2007), but its nature as a function of wavelength has not been fully investigated, nor have the consequences for QPP studies have not been fully realized. LYRA observations offer an opportunity to better understand this aspect of flares in a new wavelength regime (Aschwanden et al. 1998 and McAteer et al. 2007 both primarily studied hard X-rays) and to compare with

observations of quiet-Sun regions and active regions. Additionally, the traditional white-noise assumption used in many analysis techniques to search for QPP is invalidated. In future work, we intend to address this problem by following the techniques discussed in Vaughan (2005, 2010), and Gruber et al. (2011).

5. Preliminary conclusions and planned future work

The scientific research that was initiated with this Proba-2 Guest Investigation remains ongoing. The preliminary results obtained to date are a promising basis for future work, some of which will be carried out in collaboration with Dr Jack Ireland, another former Proba-2 Guest Investigator. In this context we will make use of the LYRA time series download and analysis tools developed within the SunPy framework by Dr Ireland. It is anticipated that the end result will be at least one publication, and likely more.

Interim results and conclusions:

- We have constructed an event list of 111 solar flares co-observed by LYRA and RHESSI.
- We have developed a technique we term 'correlation persistence mapping', essentially a windowed method for studying changes in the cross-correlation between time series.
- We have developed an automated script for querying the LYTAF database for the presence of large-angle rotations (LARs) in any input LYRA lightcurve. The script removes the affected regions in time, and splits the remaining data into sub-series. This script will be made freely available to the solar community.
- In order to ascertain the significance of red-noise effects in flares, we have conducted preliminary Fourier spectral studies of the LYRA and RHESSI time series of ~30 of the solar flares in our event list. In the majority of cases, the LYRA spectra are well-fit by a power law slope with an index of 2.0 – 2.1. RHESSI data also exhibit evidence of power-law dependence in some cases. Hence, frequency dependent noise is a **fundamental feature** of solar flares in the EUV and soft X-ray range.

Currently, a number of science issues have been identified which represent the **next steps** in this ongoing research. These include:

- Utilise fine time-cadence RHESSI data. Although default RHESSI time binning is 4s, in principle any desired time cadence may be used, but the 4s rotation period of the spacecraft and attenuator state changes must be manually accounted for. For this study, fine time resolution to enable more detailed Fourier spectra is ideal. Hence we will utilize Fourier filtering to remove frequencies corresponding to the 4s rotation from the RHESSI lightcurves.

- Refinement of the power-law fitting procedure, which is performed via a Bayesian MCMC method. This will then be applied consistently to all 111 flares in the event list, applying the LAR time series filtering script (Section 2.1) to remove Proba-2 spacecraft rotation artifacts.

- Compare current flare spectrum results with off-pointed LYRA data to get a better idea of instrumental noise effects and their contribution to the Fourier spectrum. Additionally, we will compare current flare spectrum results with quiet-Sun LYRA time intervals.

- Investigate the significance of a Fourier power law slope of 2.0 – 2.1 and its relation to the power law spectra during quiet Sun observations, and with observations throughout the EM

spectrum. This information can be used to understand the amount of 'memory' in the flare system and to probe the flare reconnection region.

- Implement a search for QPP in the red-noise corrected power spectra, following the suggested techniques of Vaughan (2010), Gruber et al. (2011). By adopting a Bayesian analysis technique, correctly accounting for the red noise background, and applying this to the full event list, we can present a **robust analysis of the true prevalence of statistically significant QPP in solar flares**.

- Apply the CPM method to the solar flares in the event list, comparing the observed fluctuations in the RHESSI and LYRA lightcurves and establishing whether there are substantive trends in the lag between flare signatures at different wavelengths. **This comparison can be carried out for both QPP and non-QPP events.** For non-QPP events, we will gain important information as to the relationship between red noise processes in flares at different wavelengths.

6. References

Aschwanden, M. et al, ApJ, 505, 941, 1998
Dolla, L. et al, ApJ, 749, 16, 2012
Gruber, D. et al., A&A, 533, 61, 2011
Inglis, A. R. & Gilbert, H. R., ApJ, accepted, 2013
Inglis, A. R. & Dennis, B. R., ApJ, 748, 139, 2012
McAteer, R. T. J. et al, ApJ, 662, 691, 2007
Vaughan, S., A&A, 431, 391, 2005
Vaughan, S., MNRAS, 307, 20, 2010